Original Paper

Cellular Physiology and Biochemistry

Cell Physiol Biochem 2011;27:401-410

Accepted: February 24, 2011

Extracellular Alkalinization Stimulates Calcium-activated Chloride Conductance in Cystic Fibrosis Human Airway Epithelial Cells

Tamás Dankó, Dóra Hargitai, Ágnes Pataki, Hasif Hakim, Miklós Molnár* and Ákos Zsembery

Institute of Human Physiology and Clinical Experimental Research, Semmelweis University, Budapest, *Institute of Pathophysiology, Semmelweis University, Budapest

Key Words

Extracellular pH • Sodium • Zinc • Ca^{2+} entry • Cl^- channels

Abstract

Background: The pH of the airway surface liquid (ASL) plays a pivotal role in maintaining the proper function of the respiratory epithelium. In patients with cystic fibrosis (CF) acidic ASL has been observed. Thus, alkalinization of ASL itself might be beneficial in CF. The aim of this study was to investigate the role of extracellular pH (pH_o) on the alternative Ca^{2+}-activated Cl^- channels (CaCCs) in CF airway epithelial cells. Methods: The $[Ca^{2+}]_i$ and viability of CF airway epithelial cells (IB3-1) were assessed using Fluo-3/AM and YO-PRO-1 fluorescent dyes, respectively. Ion currents were detected in whole-cell configuration using the patch clamp technique. Results: Extracellular alkalinization (pH_o 8.2) stimulated Ca^{2+} entry and inward currents in low Na^+ containing medium. The inward currents were blocked by the removal of extracellular Ca^{2+}, chelating cytosolic Ca^{2+}, as well as by the application of niflumic acid and DIDS. While Zn^{2+} promoted sustained Ca^{2+} entry in pH_o-dependent manner, it inhibited the anion conductance. The low external Na^+ concentrations and alkaline pH_o were well tolerated by the cells. Conclusions: Stimulation of CaCCs could be achieved by alkalinization of the extracellular environment in CF airway epithelial cells. Zn^{2+} directly blocked, however indirectly enhanced the activity of Cl^- conductance.

Copyright © 2011 S. Karger AG, Basel

Introduction

Mucociliary clearance (MCC) is the primary line of defense against bacterial infections in the airways. Its function is strongly dependent on the volume, ionic composition and pH of airway surface liquid (ASL). The normal ASL homeostasis is predominantly determined by the CFTR protein, a cAMP-regulated Cl^- channel that allows for the secretion of Cl^- and/or HCO_3^- into the luminal side of the epithelium. Apart from its secretory function, the activated CFTR also inhibits the amiloride-sensitive epithelial Na^+ channel (ENaC), reducing the reabsorption of Na^+ [1]. The basic defect in cystic fibrosis (CF) is the lack of functional CFTR proteins in the apical membrane of secretory epithelia. Therefore, cystic fibrosis airways exhibit Cl^-/HCO_3^- hyposecretion and Na^+ hyperabsorption which lead to the depletion of ASL volume resulting in reduced MCC and chronic infections of the airways [2].

KARGER

Fax +41 61 306 12 34
E-Mail karger@karger.ch
www.karger.com

© 2011 S. Karger AG, Basel
1015-8987/11/0274-0401$38.00/0

Accessible online at:
www.karger.com/cpb

Tamás Dankó MD and Ákos Zsembery MD, PhD
Institute of Human Physiology and Clinical Experimental Research,
Semmelweis University, Tûzoltó utca 37-47, 1094 Budapest (Hungary)
Tel. +36 20 6660339, Fax +36 1 334-3162
E-Mail tamas.danko@eok.sote.hu and E-Mail akos.zsembery@eok.sote.hu

The calcium-activated chloride channel (CaCC) has often been referred to as the alternative Cl^- channel, because it may provide a parallel route for Cl^- secretion across the apical membrane in tissues that lack CFTR [3]. Interestingly, the CF mouse lung appears to exhibit normal ASL homeostasis, mucus clearance, and as a consequence, no disease. A reasonable explanation for this lack of pathology is that murine airways utilize CaCCs rather than CFTR as the principal pathway for Cl^- secretion [3, 4]. In human airways, CaCCs play only a minor role in basal ASL homeostasis rather function as an acute regulator of Cl^- secretion and ASL height, integrating varying extracellular stimuli [3, 5]. Although CaCC expression appears to be up-regulated in CF, it is not able to compensate for the ion transport defects resulting from the lack of CFTR due to its relatively low basal activity [6].

Recently, two novel types of proteins could be associated with Ca^{2+}-dependent Cl^- channel function: the bestrophin family and TMEM16A (anoctamin1, ANO1). The identification of TMEM16A now provides an opportunity to better understand the fine tuning of ASL production and also, offers a primary target for the therapy of CF lung disease [7, 8].

Activation of CaCCs requires cytosolic Ca^{2+} concentrations ($[Ca^{2+}]_i$) in the range of 0.2 - 5 μM and involves either direct Ca^{2+}-binding or indirect Ca^{2+}-dependent phosphorylation of the channel protein, depending on the cell type in which it is expressed [9]. Current strategies to open CaCCs in airway epithelial cells are based on Ca^{2+} mobilization from intracellular stores and/or Ca^{2+} entry from extracellular space. One of the most common approaches is the stimulation of a Ca^{2+}-dependent Cl^- conductance via a $P2Y_2$ receptor-mediated increase of $[Ca^{2+}]_i$ [10].

Our group has previously shown that stimulation of airway epithelial cells with zinc (in the presence or absence of ATP) leads to a sustained increase in both $[Ca^{2+}]_i$ and Cl^- secretion [11, 12]. These Zn^{2+}-induced responses were strongly dependent on extracellular pH (pH_o) and Na^+ concentration. Zn^{2+} is an important biological trace element and is a crucial structural or functional component of hundreds of important proteins such as different metalloenzymes and "zinc-finger" containing proteins. However, the therapeutic application of Zn^{2+} raises several issues, because overexposure to Zn^{2+} can be harmful and leads to various side effects [13-17].

In this paper we provide evidences that elevation in pH_o *per se* is an effective activator of CaCCs in CF airway epithelial cells, without the additional application of any previously investigated agonists such as ATP or Zn^{2+}.

Materials and Methods

Cell culture

IB3-1 is a CF human bronchial epithelial cell line carrying two different mutations of the CFTR gene (ΔF508/W1282X). Cells were grown in plastic tissue culture flasks in DMEM/F12 (1:1) medium supplemented with 5% FBS, 100 U/ml penicillin and 100 μg/ml streptomycin at 37°C in a humidified cell culture incubator supplied with 5% CO_2. Cells were subcultivated when confluency reached 90-95%.

Live cell calcium imaging

For measurements of cytoplasmic Ca^{2+}-concentration, IB3-1 cells were plated at 10^6 cells/dish density on round glass coverslips (42 mm in diameter) in 60 mm dishes and were used for experiments within 24-48 hours. Cells were loaded with Fluo-3/AM (4 μM) in standard extracellular solution for 60 minutes at room temperature. Next, coverslips were mounted on the stage of an inverted microscope equipped with a perfusion chamber. At the beginning of each experiment, cells were superfused with standard extracellular solution. Standard extracellular solution contained (in mM): 145 NaCl, 5 KCl, 3 $CaCl_2$, 1 $MgCl_2$, 10 D-glucose and 10 mM HEPES, pH 7.4 (with NaOH). Sodium-free solutions contained (in mM): 145 NMDG-Cl, 5 KCl, 3 $CaCl_2$, 1 $MgCl_2$, 10 D-glucose and 10 mM HEPES, varying pHs were adjusted by either NMDG or HCl. Nominally Ca^{2+}-free solutions were prepared by simply omitting $CaCl_2$. During recordings the pH_o was altered by changing the bath solution for a buffer with the same ionic composition except for the pH. Solutions were delivered by continuous perfusion at a rate of 3 ml/min. Recordings were made with a confocal laser scanning microscope, Axiovert 200M Zeiss LSM 510 Meta (Carl Zeiss, Jena, Germany) equipped with an 20x Plan Apochromat (NA = 0,80) DIC objective. For excitation, 488-nm argon-ion laser was used. The emitted light was collected by BP 505-570 band pass filter. Data were obtained at a rate of 0.5 Hz. Changes in $[Ca^{2+}]_i$ are displayed as the percentage of fluorescence relative to the intensity at the beginning of each experiment. The baseline fluorescence (100 %) was calculated from the average fluorescence of ROIs during superfusion of cells with standard bathing solution. Background fluorescence was subtracted from readings by measuring a cell-free area on the same coverslip. All experiments were performed at room temperature.

Electrophysiology

Voltage-clamp recordings were carried out in the standard whole-cell configuration using an Axopatch 200B amplifier (Axon Instruments) [18]. Currents were monitored at -80 mV using ramp commands (-100 mV to +100 mV in 200 ms, 1mV/ms) applied every 10 s. The holding potential was -50 mV between ramps. Stable recordings were maintained for 20-30 min. Once a steady-state current was obtained, I/V relationships were determined

Fig. 1. Representative traces showing the effects of different pH_o on $[Ca^{2+}]_i$ in IB3-1 cells. Panel A: The effect of extracellular alkalinization (pH_o 8.2) on $[Ca^{2+}]_i$ in the presence of $CaCl_2$ (3 mM). In the presence of Na^+, no change was detected in $[Ca^{2+}]_i$. Panel B: The effect of varying pH_o in the presence of $CaCl_2$ (3 mM) and following the withdrawal of Na^+. Panel C: Effect of alkalinization (pH_o: 8.2) on $[Ca^{2+}]_i$ in IB3-1 cells perfused with Na^+-free medium in the presence (3 mM) and in the absence of $CaCl_2$ (nominally Ca^{2+}-free). Panel D: the effect of removal of Ca^{2+} (from 3 mM to nominally Ca^{2+}-free) during alkalinization (pH_o: 8.2) in the absence of sodium. Each trace represents the sum of approx. 40 cells in one field of view. The fluorescence intensity of the trace prior to the application of any agonist/ modification was considered as 100%. Each experiment was performed 5 times using cells from at least two different passages with similar results.

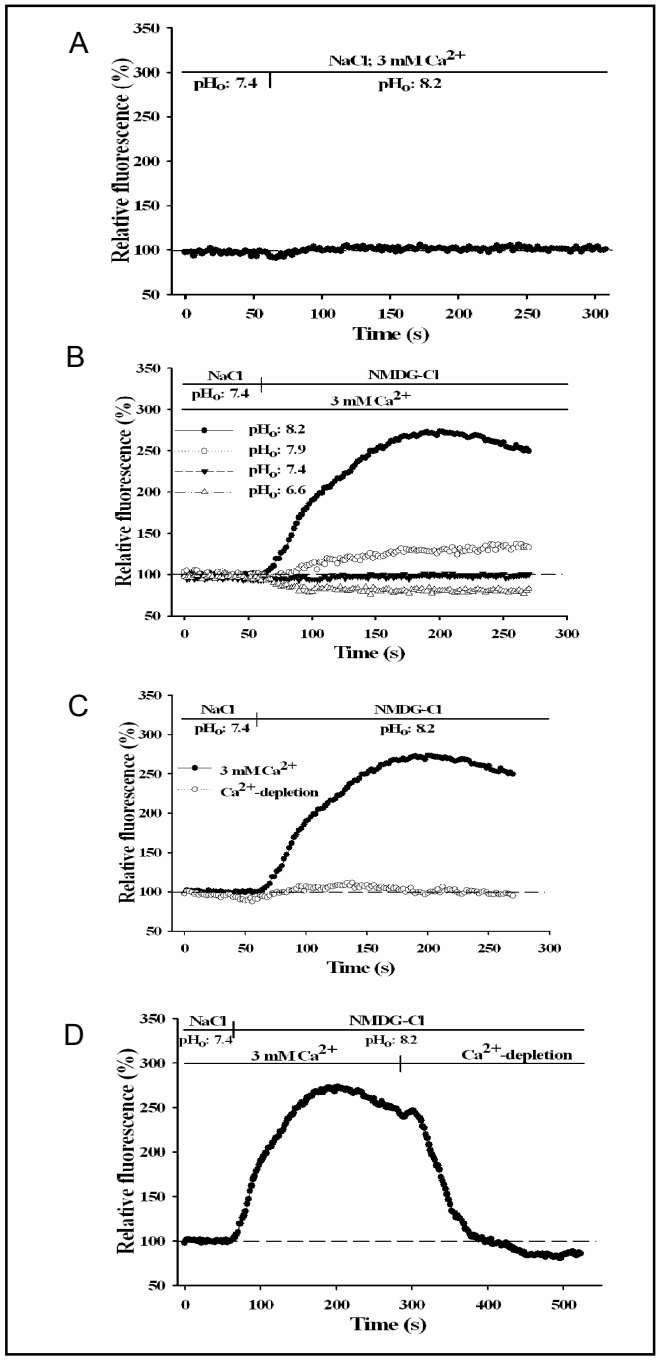

using a protocol that consisted of 300 ms square pulses of the test potential (-100 mV to +100 mV) from a holding potential of -50 mV in 20-mV increments, with 1-second intervals (polarity given for cell interior). All reported currents were normalized by cell capacitance and expressed as current density (pA/pF). Command protocols and data acquisition were controlled by pClamp 6.03 software (Axon Instruments). Capacitative currents were compensated with analog compensation. Linear leak currents were not compensated. Series resistance was accepted if lower than five times the pipette tip resistance. Analog data were filtered at 1 kHz with a low-pass Bessel filter and digitized at 5kHz using a Digidata 1200 interface board. Membrane potentials were corrected for liquid junction potential if greater than 2 mV values were detected. Micropipettes were pulled by a P-97 Flaming-Brown type micropipette puller (Sutter Instrument) from borosilicate glass capillary tubes (Harvard Apparatus) and had a tip resistance of 3–6 MΩ when filled with pipette solution. Standard pipette solution contained (in mM): 140 NMDG-Cl, 1 $MgCl_2$, 2 EGTA, 10 HEPES, pH 7.2 (with NMDG) and an appropriate concentration of $CaCl_2$, to give free $[Ca^{2+}]_i$ = 0.1 μM. In some experiments high free $[Ca^{2+}]_i$ = 1 μM was used. Free $[Ca^{2+}]_i$ was estimated using MaxChelator software (Stanford University). Low intracellular Cl^- solution contained (in mM): 90 NMDG-glutamate, 50 NMDG-Cl, 1 $MgCl_2$, 2 EGTA, 10 HEPES, pH 7.2 with NMDG (free $[Ca^{2+}]_i$ = 0.1 μM). Increased Ca^{2+}-buffering pipette solution contained (in mM): 140 NMDG-Cl, 1 $MgCl_2$, 20 EGTA, 10 HEPES, pH 7.2 (with NMDG). Standard extracellular solution contained (in mM): 145 NaCl, 2 $CaCl_2$, 1 $MgCl_2$, 10 D-glucose, 10 HEPES, pH 7.4 (with NaOH). Na^+-free control extracellular solution contained (in mM): 145 NMDG-Cl, 1 $MgCl_2$, 10 D-glucose, 10 HEPES, pH 7.4 (with NMDG) and 3 $CaCl_2$, unless stated otherwise. In some experiments, NaCl was equimolarly replaced by either TRIS-Cl or CsCl. After whole cell configuration was obtained in standard solution, bath solution was immediately switched to Na^+-free control solution. After 3-5 min (time for proper dialysis of the cell interior) experimental protocols were initiated. Niflumic acid (NFA) was added to the bath solution for 5 min before initiating any experimental protocol. All solutions were delivered by continuous perfusion with a gravity-fed delivery system. All experiments were performed at room temperature.

YO-PRO-1 permeability assay

Fluorescence was detected using a Zeiss LSM 510 META laser scanning microscope. YO-PRO-1 (MW: 629) fluorescence was measured from single cells in the field of view (usually 20–40 cells with 20X objective). Excitation and emission wavelengths were 480 nm and 509 nm, respectively. YO-PRO-1 (1 μM) was continuously present in all solutions before and during agonist application. Images were captured at 0.5 Hz. YO-PRO-1 fluorescence from individual cells was averaged to obtain mean response. All experiments were performed at room temperature.

Fig. 2. Alkaline pH_o-induced whole cell currents in the absence of extracellular Na^+. Panel A: time course of inward current induced by alkalinization (pH_o: 8.2) in the presence of 3 mM $CaCl_2$, when extracellular Na^+ was substituted with $NMDG^+$. Currents were measured every 10 s at -80 mV during voltage ramps ranging from -100 to 100 mV in 200 ms. Standard pipette solution was used. Panel B: original traces demonstrating current-voltage relationships during voltage ramps at pH_o: 7.4 and at pH_o: 8.2, measured at time points indicated in panel A (arrows). Panel C: Once steady-state current was obtained (indicated by arrows on panel A), voltage-step protocol (see materials and methods) was applied. The resultant currents are shown as representative traces. Panel D: I/V relationships showing summarized data of steady-state currents at varying pH_o (6.6, 7.4, 7.9, 8.2) in the absence of extracellular Na^+. Data represent means ± S.E. from 6-12 cells. Panel E: comparison of inward currents induced by extracellular alkalinization (pH_o: 8.2) in the presence of four different main extracellular cations, when NMDG-Cl is equimolarly replaced with TRIS-Cl, CsCl and NaCl (145 mM each). Currents are plotted relative to currents elicited in the presence of NMDG-Cl, *$p < 0.05$. Panel F: comparison of alkalinization-induced inward currents in extracellular solutions containing different concentrations of Na^+. To maintain the constant ionic strength in the solutions, NMDG-Cl was equimolarly replaced with NaCl. Currents are plotted relative to currents elicited in the absence of Na^+, *$p < 0.05$.

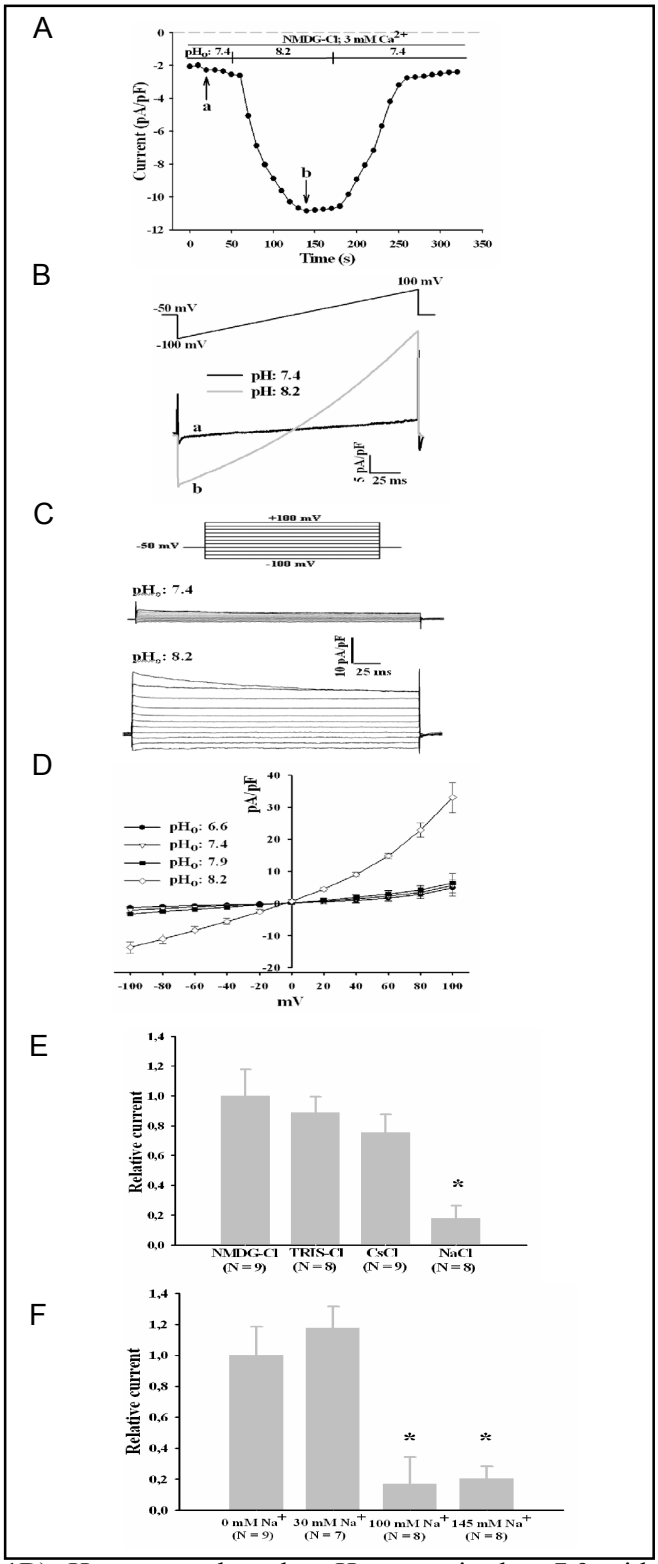

Data presentation

Results were presented as means ± S.E. of N observations. Statistical significance was determined using paired Student's t-test. Differences were considered statistically significant when $p < 0.05$.

Materials

NFA, DIDS, $ZnCl_2$ and Triton X-100 (TX-100) were purchased from Sigma Chemical (St. Louis, MO). Fluo-3/AM and YO-PRO-1 iodide were purchased from Invitrogen Inc. (Carlsbad, CA). All other chemicals were purchased from Csertex Inc. (Budapest, Hungary).

Results

Effects of extracellular pH on intracellular calcium concentrations in IB3-1 cells

In the presence of Na^+ (145 mM) alkalinization of pH_o (from 7.4 to 7.9 or 8.2) did not cause significant alterations in basal $[Ca^{2+}]_i$ (NaCl pH_o 7.4: 101.7 ± 0.7 % [N=16] vs. NaCl pH_o 8.2: 101.8 ± 2.3 % [N=5] p=n.s) (Fig. 1A). In subsequent experiments, extracellular Na^+ was substituted by a non-permeant large organic cation N-methyl-D-glucamine ($NMDG^+$). At pH_o 7.4, acute removal of external Na^+ did not cause a change in basal Ca^{2+} level (NaCl pH_o 7.4: 101.7 ± 0.7 % [N=16] vs. NMDG-Cl pH_o 7.4: 101.9 ± 1.1 % [N=5] p=n.s) (Fig. 1B). However, when the pH_o was raised to 7.9 with parallel replacement of extracellular Na^+, a mild but sustained elevation in intracellular Ca^{2+} levels could be observed (NaCl pH_o 7.4: 101.7 ± 0.7 % [N=16] vs. NMDG-Cl pH_o 7.9: 133.5 ± 3.5 % [N=5] $p < 0.05$) (Fig. 1B) Raising pH_o to a higher level (from 7.4 to 8.2) elicited

a markedly greater increase in intracellular calcium levels that reached a plateau within the first 3 minutes (NaCl pH_o 7.4: 101.7 ± 0.7 % [N=16] vs. NMDG-Cl pH_o 8.2: 239.8 ± 13.3 % [N=5] $p < 0.05$) (Fig. 1B). To investigate whether the increase in $[Ca^{2+}]_i$ was due to Ca^{2+} entry, we repeated the experiments with nominally Ca^{2+}-free solutions. Under these experimental conditions cells failed to respond with an increase in $[Ca^{2+}]_i$ (3 mM $CaCl_2$: 239.8 ± 13.3 % [N=5] vs. Ca^{2+}-depleted solution: 107.6 ± 1.1 % [N=5] $p < 0.05$ at pH_o 8.2 in the presence of NMDG-Cl) (Fig. 1C). Furthermore, withdrawal of extracellular Ca^{2+} during alkalinization abolished the sustained elevation of $[Ca^{2+}]_i$ suggesting that Ca^{2+} originated from extracellular sources (Fig. 1D). In contrast to the effects of extracellular alkalinization, lowering the pH_o (from 7.4 to 6.6) in the absence of extracellular Na^+ caused a mild, but sustained decrease in $[Ca^{2+}]_i$ (NaCl pH_o 7.4: 101.7 ± 0.7 % [N=16] vs. NMDG-Cl pH_o 6.6: 85.9 ± 2.4 % [N=5] $p < 0.05$) (Fig. 1B), whereas had no effect at all in the presence of Na^+ (data not shown).

Effects of extracellular pH on whole-cell currents in the presence of different monovalent cations

Whole-cell configuration was obtained in normal extracellular solution. Control currents were recorded following substitution of external Na^+ by $NMDG^+$. At pH_o 8.2, we observed a slowly activating, large inward current that reached a plateau in approx. 2 min. This current was fully reversible upon resetting the pH_o to 7.4, and reversed near the equilibrium potential of Cl^- ($E_{rev.}$ = -3.2 ± 0.7 mV [N=8] vs. E_{Cl}^- = -1.9 mV) (Fig. 2A-C). Following partial replacement of intracellular Cl^- with glutamate (see materials and methods), the reversal potential of the alkaline pH_o-induced current remained close to that of E_{Cl}^- (E_{rev}: -25.9 ± 1.7 mV [N=5] vs. E_{Cl}^-: -28.7 mV). These data suggest that inward currents measured at -80 mV represent chloride efflux. Moderate increase in pH_o (7.9) did not elicit significant change in inward currents (Fig. 2D). In order to show whether this stimulatory effect was not specific for $NMDG^+$, we replaced Na^+ with either $TRIS^+$ or Cs^+. Under these circumstances, alkaline pH_o (8.2) elicited a similar increase in inward current compared to that observed in the presence of $NMDG^+$, suggesting that this effect was independent of the nature and permeability features of the substituting cations (Fig 2E). Additionally, the complete absence of Na^+ is a non-physiological condition; therefore, we tested the effects of alkaline pH_o at various extracellular Na^+ concentrations. External alkalinization did not elicit an increase in inward currents when external Na^+ concentration was near to

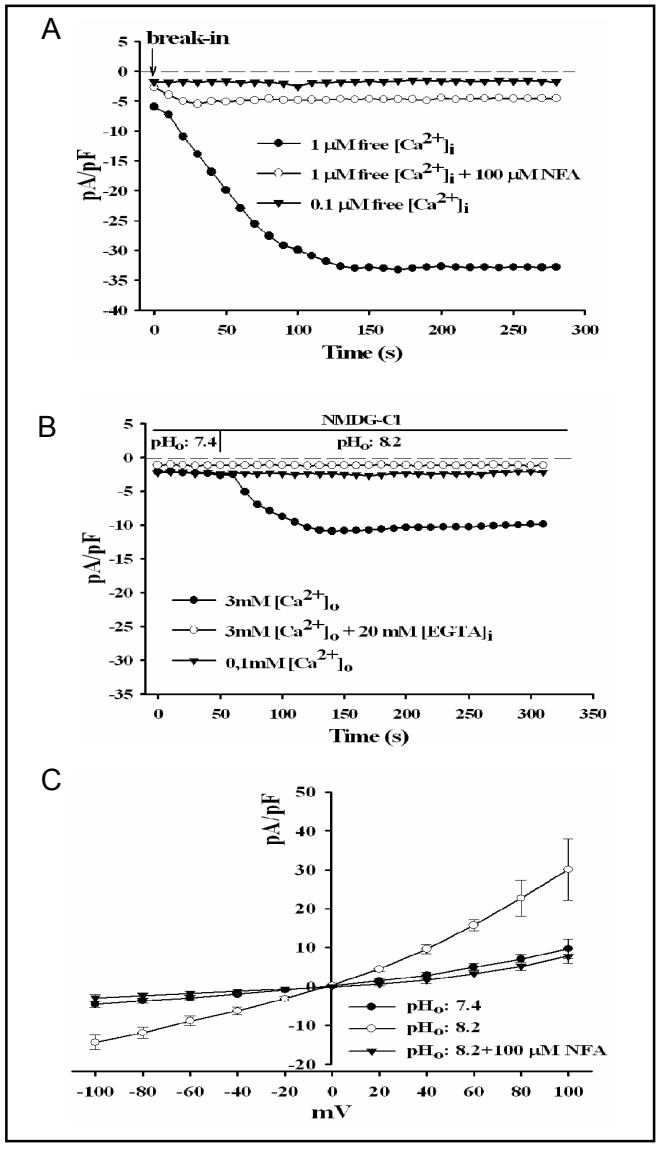

Fig. 3. Calcium-activated chloride channels are involved in alkaline pH_o-induced inward currents. Panel A: Demonstration of a Ca^{2+}-induced Cl^- conductance in IB3-1 cells. Time course of inward currents after cells were dialyzed with either 0.1 μM or 1 μM free $[Ca^{2+}]_i$ containing pipette solution. Cells were continuously perfused with Na^+-free control extracellular solution. In some experiments, NFA (100 μM) was added to the bath 5 min before whole cell formation (*break-in*). Currents were measured every 10 s at -80 mV during voltage ramps ranging from -100 to 100 mV in 200 ms. Representative traces are shown. Panel B: calcium dependency of inward currents induced by alkaline pH_o (8.2) in the absence of extracellular Na^+, but in the presence of 3 mM extracellular Ca^{2+}. Pipettes were filled either with standard or high Ca^{2+}-buffering (20 mM $[EGTA]_i$) intracellular solution. Experiments were also performed in Ca^{2+}-depleted (0.1 mM) extracellular solution (with standard pipette solution). Panel C: summarized data showing the effect of the anion channel blocker NFA (100 μM) on the alkalinization-induced currents. Pipettes were filled with standard solution. Data represent means ± S.E. from 6-12 cells.

Fig. 4. Effect of zinc on calcium-activated chloride channel activity in IB3-1 cells. Panel A: Representative traces showing the effect of pH_o on the Zn^{2+}-induced Ca^{2+}-signal in Na^+-free external solution. First, pH_o was changed to either 6.6 (open circles) or 8.2 (filled circles) with parallel substitution of extracellular Na^+ by $NMDG^+$ (in the presence of 3 mM $CaCl_2$). The cells were then challenged with 20 μM $ZnCl_2$ and the pattern of the Ca^{2+} signal was recorded. Panel B: time course of inward currents induced either by alkalinization (filled circles) or by the simultaneous application of alkaline pH_o and 20 μM $ZnCl_2$ (open circles) in the absence of extracellular Na^+. Currents were measured every 10 s at -80 mV during voltage ramps ranging from -100 to 100 mV in 200 ms. Standard pipette solution was used. Panel C: Summarized data showing the maximal change in current amplitude detected at -80 mV during voltage ramps in the presence and absence of 20 μM $ZnCl_2$ according to results in Panel B, *$p < 0.05$. Panel D: the effect of 20 μM $ZnCl_2$ on Ca^{2+}-induced Cl^- currents induced by inclusion of 1 μM free $[Ca^{2+}]_i$ in the pipette solution. Zn^{2+} was applied at time point indicated by the arrow. Currents were measured every 10 s at -80 mV during voltage ramps ranging from -100 to 100 mV in 200 ms. Panel E: bar graph showing the effect of pretreatment with $ZnCl_2$ (5 min, 20 μM) on peak current amplitude detected at -80 mV during voltage ramps, when pipette solution contained 1 μM free $[Ca^{2+}]_i$, *$p < 0.05$.

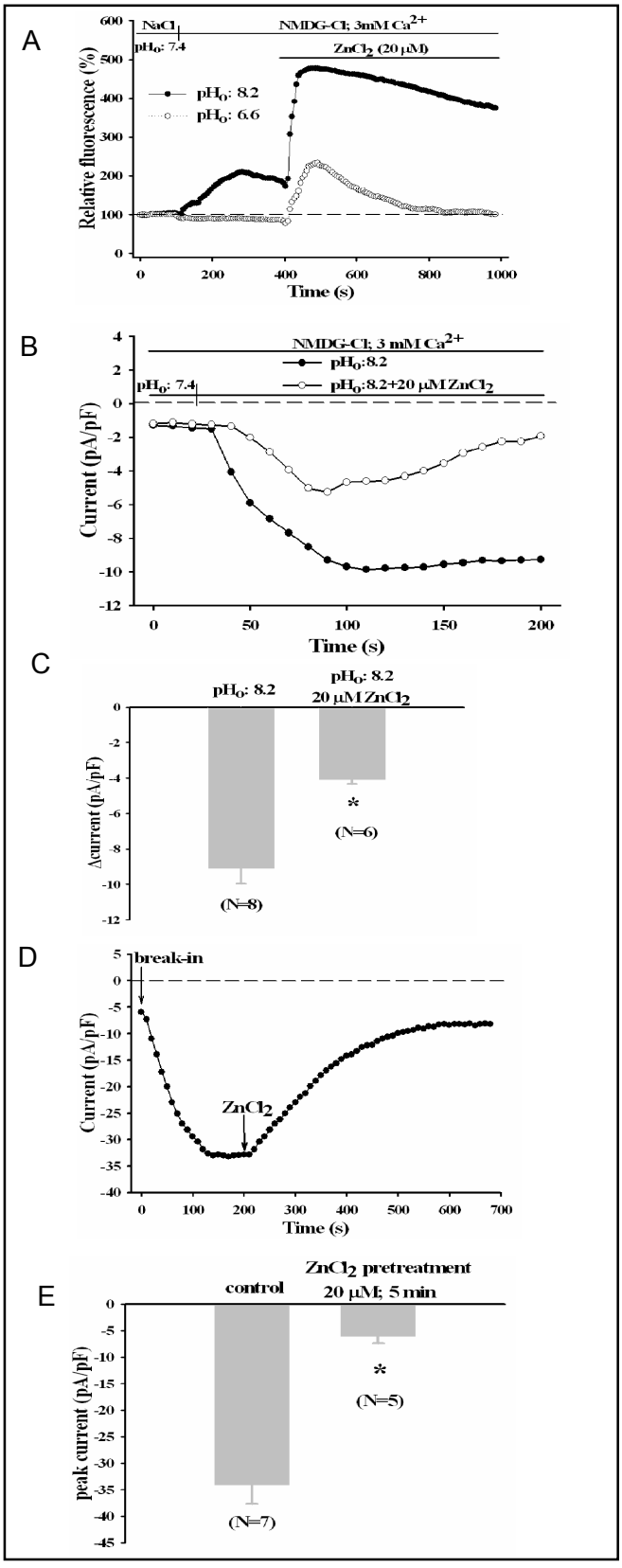

physiological values (Fig. 2F). These data are in agreement with our Ca^{2+} imaging data. In contrast, acidification of pH_o (6.6) resulted in a slight decrease in inward currents (Fig. 2D).

Inward current is due to stimulation of calcium-activated chloride channels

First, we aimed to demonstrate the presence of CaCCs in IB3-1 cells. The cell interior was dialyzed with pipette solution containing high (1 μM) free $[Ca^{2+}]_i$. Under these conditions we observed a significantly higher peak inward current compared to that obtained with standard (0.1 μM free $[Ca^{2+}]_i$) pipette solution (-2.1 ± 0.1 pA/pF [N=15] vs. -34.2 ± 3.5 pA/pF [N=7] $p < 0.05$ at -80 mV) (Fig. 3A). The resulting increase in current was prevented by 100 μM NFA, a potent inhibitor of CaCCs (-34.2 ± 3.5 pA/pF [N=7] vs. -4.6 ± 0.5 pA/pF [N=5] $p < 0.05$ at -80 mV) (Fig. 3A). To test whether CaCCs were involved in the alkaline pH_o-induced increase of inward current, we first examined the dependency on external calcium. In NMDG-rich solution, at pH_o 8.2 the peak inward current (-11.0 ± 1.4 pA/pF [N=8] at -80 mV) was reduced when experiments were performed either in extracellular solution containing 0.1 mM Ca^{2+} (-2.1 ± 0.1 pA/pF [N=15] $p < 0.05$ at -80 mV) or by the application of 20 mM EGTA in the pipette solution (-1.1 ± 0.1 pA/pF [N=6] $p < 0.05$ at -80 mV) (Fig. 3B). These results indicate that Ca^{2+} entry from extracellular space plays a crucial role in the activation of the whole-cell inward currents in these CF airway epithelial cells.

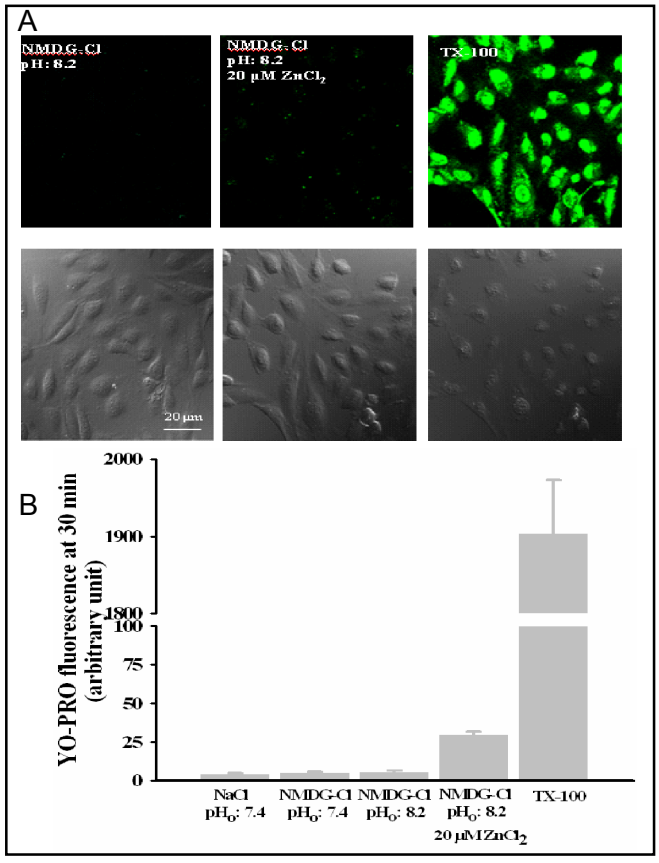

Fig. 5. Effects of alkaline pH_o and zinc on the permeability properties of IB3-1 cells. Panel A: Original images demonstrating the effect of varying extracellular conditions on the cellular uptake of YO-PRO-1. Cells were incubated in the continuous presence of YO-PRO-1 (1 μM) and 3 mM $CaCl_2$ in either Na^+-free alkaline (pH_o: 8.2) solution (*top left*), or with the simultaneous application of 20 μM $ZnCl_2$ (*top middle*) for 30 min at room temperature. The lack of YO-PRO-1 fluorescence in the cells (neither cytoplasmic, nor nuclear) indicates that the cells remain intact during our experimental conditions. *Top right* image: at the end of each experiment, 5 μl/ml of the permeabilizing agent TX-100 was added to the bath solution to initiate the entrance of YO-PRO-1 into the cells as it is confirmed by the strong nuclear labeling. *Bottom left, middle and right:* corresponding phase contrast images of the cells. Panel B: Summary of steady-state YO-PRO-1 fluorescence measured at 30 min in the presence of different extracellular conditions. Note the break and change in scale required for TX-100. Each bar represents the mean ± SE of 4-6 experiments.

Next, we tested whether NFA was able to inhibit the alkaline pH_o-induced inward current. As shown in Figure 3C, the inward current was totally blocked by pretreatment with 100 μM NFA, suggesting the involvement of CaCCs. In order to confirm these data, we used another inhibitor of Cl^- channels, DIDS (200 μM) which inhibited the inward current as well (data not shown).

Effects of zinc on calcium-activated chloride currents

Our research group has already investigated the effects of low micromolar Zn^{2+} (20 μM) in IB3-1 cells in the range of pH_o 7.3-7.9. We have previously found that in a Na^+-free, alkaline (pH_o 7.9) environment, Zn^{2+} elicited a sustained increase in $[Ca^{2+}]_i$, while in the presence of Na^+, zinc failed to induce changes in Ca^{2+} level regardless of pH_o [12]. Therefore, we tested Zn^{2+}-induced Ca^{2+} entry represented by the plateau phase of the Ca^{2+} signal at both pH_o 6.6 and 8.2 in the absence of Na^+. As shown in Fig. 4A, at alkaline pH_o (8.2) Zn^{2+} elicited a sustained Ca^{2+} plateau, while at acidic pH_o (6.6) we observed only a transient increase in Ca^{2+} signal. These data indicate that Zn^{2+} promotes Ca^{2+} entry in a pH_o-dependent manner.

Subsequently, we tested the effects of Zn^{2+} on CaCC-mediated Cl^- currents. When cells were perfused with a Na^+ -free, alkaline solution in the presence of $ZnCl_2$ (20 μM), inward currents were transient and the maximal amplitude reached only approx. half the value of the current that we observed in the absence of Zn^{2+} (Fig. 4B, C). We hypothesized that this effect of Zn^{2+} was due to direct inhibition of CaCCs. Indeed, application of Zn^{2+} (20 μM) exerted a strong inhibitory effect on steady-state currents induced by high (1 μM) free $[Ca^{2+}]_i$ containing pipette solution. (Fig. 4D) Additionally, the inward current evoked by 1 μM free $[Ca^{2+}]_i$ was prevented by 5 min pretreatment with 20 μM Zn^{2+} (Fig. 4E). Taken together, these data show that although Zn^{2+} stimulates Ca^{2+} entry in airway epithelial cells it also effectively inhibits CaCCs.

Effects of alkaline pH and zinc on cell viability

The continuous presence of alkaline pH_o, Zn^{2+} and the sustained increase in $[Ca^{2+}]_i$ may induce apoptosis of cells that can essentially be characterized by increased membrane permeability for large molecules such as the green fluorescent dye, YO-PRO-1. Therefore, we used the YO-PRO-1 uptake assay to examine the permeability properties of IB3-1 cells during exposure to high pH_o and Zn^{2+}. As it is shown in Fig. 5, neither elevations in pH_o alone, nor in concert with low micromolar (20 μM) Zn^{2+} caused a considerable increase in membrane permeability for the large YO-PRO-1 molecule during the 30 min incubation time, as compared to the prompt effect of the permeabilizing agent TX-100 (Fig. 5A, B). These data suggest that exposure to these conditions can be well tolerated and does not lead to cell death within the investigated period.

Discussion

The present study has three major findings. First, in CF airway epithelial cells, alkaline pH_o (8.2) elicited Ca^{2+} entry in Na^+-free environment. Second, the alkaline pH_o-induced increase in $[Ca^{2+}]_i$ resulted in the activation of Ca^{2+}-dependent Cl^- currents. These currents exhibited strong dependence on extracellular Ca^{2+} concentration and were inhibited by NFA, a known blocker of CaCCs. Third, Zn^{2+} inhibited CaCCs while it enhanced Ca^{2+} entry at alkaline pH_o.

Due to the absence or dysfunction of the cAMP/PKA-regulated CFTR Cl^- channels, the CF airway epithelium exhibits a reduced capacity to secrete Cl^- and water to the airway surface. Furthermore, an increased reabsorption of Na^+ contributes to dehydration of the thin fluid layer above the airway epithelial cells resulting in impaired mucociliary clearance [19, 20]. Therefore, pharmacotherapeutic interventions aimed to stimulate alternative CaCCs and/or inhibit ENaCs are under development. It is noteworthy that the UTP analog Denufosol has been shown to stimulate purinergic $P2Y_2$ receptors increasing the rate of PIP_2 hydrolysis that resulted in IP_3-dependent release of Ca^{2+} from intracellular stores [21]. The increase in free $[Ca^{2+}]_i$ activated chloride secretion through CaCCs, while depletion in PIP_2 levels led to the decrease in ENaC activity. Consequently, aerosolized Denufosol appeared to be highly beneficial for CF patients during clinical Phase I and II studies and the completion of Phase III trials is underway. Another drug, Moli-1901 (duramycin) is currently in Phase II clinical trials in Europe. This peptide interacts with phospholipids present in plasma and organelle membranes, thereby elevating intracellular Ca^{2+} from both internal stores and the extracellular space which in turn leads to the activation of CaCCs [22]. In addition, spiperone, a known anti-psychotic drug applied to the "enhanced calcium transfer solution" elicited a sustained increase in $[Ca^{2+}]_i$ and stimulated CaCCs in both CF and non-CF airway epithelial cells [23].

Therapeutic interventions designed to activate CaCCs via Ca^{2+} -mobilizing agonists must face (at least) one serious problem. As it was thoroughly analyzed in Xenopus oocytes, CaCC-mediated currents display time and voltage dependent profile [24]. At intermedier (subsaturating) Ca^{2+} concentrations the voltage dependent channel inactivation (fast deactivation at negative potentials) exceeds the Ca^{2+}-dependent channel activation thereby resulting in an outwardly rectifying current-voltage relationship, and hence, no Cl^- efflux. To induce Cl^- efflux via CaCCs, intracellular Ca^{2+} concentrations should reach saturating values (>1 μM) when the Ca^{2+}-dependent channel opening becomes voltage independent with a consequently linear current-voltage plot [24]. However, we hypothesize that activation of CaCCs requires a saturating Ca^{2+} concentration only in the subplasmalemmal space. Since rate of diffusion through the plasma membrane is much faster than diffusion rate towards the center of the cell, Ca^{2+} entry from the extracellular space leads to accumulation of Ca^{2+} near the plasma membrane [25]. Furthermore, Cl^- currents show strong correlation with Ca^{2+} signals if Ca^{2+} derives from the extracellular space [25]. On the other hand, Ca^{2+} signals provided by the Ca^{2+} release from internal stores must reach markedly higher levels in the bulk cytosol to induce Cl^- efflux. In fact, large and long-lasting increases of $[Ca^{2+}]_i$ could lead to undesirable side effects, such as apoptosis and/or activation of inflammatory processes. Consequently, controlled Ca^{2+} entry through the plasma membrane might be beneficial for therapeutic purposes in CF. We have previously shown that in CF mouse nasal epithelial cells Ca^{2+} entry could be switched on/off by modifying external ionic environment [12]. In an alkaline, low Na^+-containing medium, ATP and Zn^{2+} induced sustained elevation of Cl^- secretion, an effect that was abolished by reducing pH_o or replacing external Na^+. However, under these conditions there were too many varying factors. As a result, we attempted to determine the role of different modifications of the extracellular environment separately.

Extracellular pH is a well-known modulator of plasma membrane Ca^{2+} channels and consequently the intracellular Ca^{2+} homeostasis [26]. Ca^{2+} entry can occur through voltage-dependent Ca^{2+} channels, P2X receptors, store-operated Ca^{2+} channels (SOCs), receptor-operated Ca^{2+} channels (ROC), transient receptor potential Ca^{2+} channels and Na^+/Ca^{2+} exchangers (NCX) (in reverse operation mode). With respect to their responsiveness to changes in pH_o, most of the Ca^{2+} entry mechanisms studied so far, appear to share common characteristics: extracellular acidification attenuates whereas alkalinization stimulates Ca^{2+} influx [27]. These data are in strong correlation with the early observation that transepithelial Ca^{2+} transport is inhibited in conditions associated with overproduction of acids [28]. In fact, we have found that extracellular acidification caused a mild but sustained decrease in both $[Ca^{2+}]_i$ and CaCC activity. Interestingly, in the presence of physiologic Na^+ concentrations (145 mM), alterations in pH_o did not cause significant changes in $[Ca^{2+}]_i$. These data suggest that in airway epithelial

cells, pH_o -dependent changes of Ca^{2+} homeostasis occur only in the absence of Na^+. Removal of extracellular Na^+ could induce the reverse operation mode of the NCX. However, NCX was found to be insensitive to external alkalinization between 7.3 and 9.0 [29]. Furthermore, we have previously demonstrated that IB3-1 cells did not possess NCX [12]. We also asked whether increasing the extracellular pH with parallel removal of sodium could induce a significant change in pH_i. Our unpublished observations suggested that in Na^+-free medium, increasing the external pH from 7.4 to 8.2 caused a change of pH_i less than 0.1 unit. Thus, under these conditions IB3-1 cells seem to be quite "resistant" to external alkalinization. In addition, in the patch clamp experiments we used Hepes (10 mM) in the standard pipette solution which has been shown to adequately buffer pH_i following changes in pH_o [30].

Extracellular sodium may be another important regulator of Ca^{2+} entry pathway. Previous studies suggest that extracellular Na^+ may inhibit the channels by competing with Ca^{2+} within the permeation pathway [11, 31]. In addition, Ma and his colleagues have reported that extracellular Na^+ inhibited the P2XR-mediated Ca^{2+} influx by binding to the extracellular site on the $P2X_{cilia}$ receptor in rabbit airway ciliated cells [32]. Using different substituting cations ($NMDG^+$, $Tris^+$ and Cs^+) we have abolished the Na^+-dependent inhibition of alkaline pH_o -induced Ca^{2+} influx. Our data underline the specific role of Na^+ in these processes. Thus, we suggest that increasing pH_o with a parallel decrease of extracellular Na^+ concentration effectively enhance Ca^{2+} entry. We might speculate that changes in surface potential caused by the binding of H^+ to negative charges on the cell surface are sensed by gating mechanism of Ca^{2+} permeable channels [30, 33]. If these channels are non-selective cation channels, inhibitory effects of extracellular Na^+ could also be explained. Nonetheless, investigation of the exact mechanisms of Ca^{2+} influx is beyond the scope of this study and further experiments are needed to address this question.

In our previous work we found that application of zinc either alone or with ATP caused a sustained increase in $[Ca^{2+}]_i$ that was able to induce Cl^- secretion in both *in vitro* and *in vivo* studies [12]. Extracellular Zn^{2+} is known to alter cytosolic Ca^{2+} levels by both triggering Ca^{2+} release from internal stores and interacting with receptor channels such as NMDA, GABA and/or P2X [34-36]. Furthermore, Zn^{2+} inhibits SOCs which represent an important Ca^{2+} entry pathway in non-excitable cells [37]. Our research group has recently demonstrated that extracellular ionic strength determines whether extracellular Zn^{2+} increases or decreases cytosolic Ca^{2+} levels [38]. In addition, data are contradictory regarding the effects of Zn^{2+} on epithelial chloride channels. Ca^{2+}-activated Cl^- channels are stimulated, but voltage-gated Cl^- channels (ClC-2) are inhibited by Zn^{2+} [39, 40]. All these previous observations prompted us to investigate the effects of Zn^{2+} on CaCCs. To our surprise we have found that zinc promoted Ca^{2+} entry while it inhibited CaCCs at alkaline pH_o. We hypothesize a direct interaction between zinc and the channel protein, since there is little evidence about the regulation of CaCCs by pH [9]. Thus, we assume that several factors such as concentration of Zn^{2+}, composition of external solutions and the type of anion channels might determine the net effect of Zn^{2+} on Cl^- conductance.

In conclusion, we report here that in CF airway epithelial cells, extracellular alkalinization per se could elicit Ca^{2+} entry and evoke Ca^{2+}-activated Cl^- conductance. Our data suggest that these effects are strongly dependent on external Na^+ concentrations, suggesting that composition of a saline vehicle could significantly alter the therapeutic effects of an inhaled drug. Furthermore, we suggest that Zn^{2+} could have a dual effect on Ca^{2+}-activated Cl^- conductance. We speculate that the inclusion of Zn^{2+} might be unnecessary in a sufficiently alkaline saline vehicle. These data might help to optimize the composition of aerosols used for treatment of cystic fibrosis.

Acknowledgements

This work was supported by the grant of the Hungarian Scientific Research Fund (OTKA K79189). We thank Dr. Gergely Kovács for helpful comments and discussions.

References

1 Kunzelmann K, Kathöfer S, Greger R: Na^+ and Cl^- conductances in airway epithelial cells: Increased Na^+ conductance in cystic fibrosis. Pflugers Arch 1995;431:1-9.

2 Knowles MR, Boucher RC: Mucus clearance as a primary innate defense mechanism for mammalian airways. J Clin Invest 2002;109:571-577.

3 Clarke LL, Grubb BR, Yankaskas JR, Cotton CU, McKenzie A, Boucher RC: Relationship of a non-cystic fibrosis transmembrane conductance regulator-mediated chloride conductance to organ-level disease in $Cftr^{-/-}$ mice. Proc Natl Acad Sci USA 1994;91:479-483.

4 Grubb BR, Pickles RJ, Ye H, Yankaskas JR, Vick RN, Engelhardt JF, Wilson JM, Johnson LG, Boucher RC: Inefficient gene transfer by adenovirus vector to cystic fibrosis airway epithelia of mice and humans. Nature 1994;371:802-806.

5 Tarran R, Button B, Picher M, Paradiso AM, Ribeiro CM, Lazarowski ER, Zhang L, Collins PL, Pickles RJ, Fredberg JJ, Boucher RC: Normal and cystic fibrosis airway surface liquid homeostasis. The effects of phasic shear stress and viral infections. J Biol Chem 2005;280:35751-35759.

6 Knowles MR, Clarke LL, Boucher RC: Activation by extracellular nucleotides of chloride secretion in the airway epithelia of patients with cystic fibrosis. N Engl J Med 1991;325:533-538.

7 Kunzelmann K, Kongsuphol P, Aldehni F, Tian Y, Ousingsawat J, Warth R, Schreiber R: Bestrophin and tmem16-Ca^{2+} activated Cl^- channels with different functions. Cell Calcium 2009;46:233-241.

8 Rock JR, O'Neal WK, Gabriel SE, Randell SH, Harfe BD, Boucher RC, Grubb BR: Transmembrane protein 16a (tmem16a) is a Ca^{2+}-regulated cl- secretory channel in mouse airways. J Biol Chem 2009;284:14875-14880.

9 Hartzell C, Putzier I, Arreola J: Calcium-activated chloride channels. Annu Rev Physiol 2005;67:719-758.

10 Kellerman D, Evans R, Mathews D, Shaffer C: Inhaled p2y2 receptor agonists as a treatment for patients with cystic fibrosis lung disease. Adv Drug Deliv Rev 2002;54:1463-1474.

11 Zsembery A, Boyce AT, Liang L, Peti-Peterdi J, Bell PD, Schwiebert EM: Sustained calcium entry through p2x nucleotide receptor channels in human airway epithelial cells. J Biol Chem 2003;278:13398-13408.

12 Zsembery A, Fortenberry JA, Liang L, Bebok Z, Tucker TA, Boyce AT, Braunstein GM, Welty E, Bell PD, Sorscher EJ, Clancy JP, Schwiebert EM: Extracellular zinc and atp restore chloride secretion across cystic fibrosis airway epithelia by triggering calcium entry. J Biol Chem 2004;279:10720-10729.

13 Adamson IY, Prieditis H, Hedgecock C, Vincent R: Zinc is the toxic factor in the lung response to an atmospheric particulate sample. Toxicol Appl Pharmacol 2000;166:111-119.

14 Barceloux DG: Zinc. J Toxicol Clin Toxicol 1999;37:279-292.

15 Blanc PD, Boushey HA, Wong H, Wintermeyer SF, Bernstein MS: Cytokines in metal fume fever. Am Rev Respir Dis 1993;147:134-138.

16 Davidson TM, Smith WM: The bradford hill criteria and zinc-induced anosmia: A causality analysis. Arch Otolaryngol Head Neck Surg 2010;136:673-676.

17 Kuschner WG, D'Alessandro A, Wong H, Blanc PD: Early pulmonary cytokine responses to zinc oxide fume inhalation. Environ Res 1997;75:7-11.

18 Hamill OP, Marty A, Neher E, Sakmann B, Sigworth FJ: Improved patch-clamp techniques for high-resolution current recording from cells and cell-free membrane patches. Pflugers Arch 1981;391:85-100.

19 Mall M, Grubb BR, Harkema JR, O'Neal WK, Boucher RC: Increased airway epithelial na+ absorption produces cystic fibrosis-like lung disease in mice. Nat Med 2004;10:487-493.

20 Mall MA: Role of the amiloride-sensitive epithelial Na^+ channel in the pathogenesis and as a therapeutic target for cystic fibrosis lung disease. Exp Physiol 2009;94:171-174.

21 Kellerman D, Rossi Mospan A, Engels J, Schaberg A, Gorden J, Smiley L: Denufosol: A review of studies with inhaled p2y(2) agonists that led to phase 3. Pulm Pharmacol Ther 2008;21:600-607.

22 Clunes MT, Boucher RC: Front-runners for pharmacotherapeutic correction of the airway ion transport defect in cystic fibrosis. Curr Opin Pharmacol 2008;8:292-299.

23 Liang L, MacDonald K, Schwiebert EM, Zeitlin PL, Guggino WB: Spiperone, identified through compound screening, activates calcium-dependent chloride secretion in the airway. Am J Physiol Cell Physiol 2009;296:C131-141.

24 Kuruma A, Hartzell HC: Bimodal control of a Ca^{2+}-activated Cl^- channel by different Ca^{2+} signals. J Gen Physiol 2000;115:59-80.

25 Machaca K, HC Hartzell: Reversible ca gradients between the subplasmalemma and cytosol differentially activate ca-dependent cl currents. J Gen Physiol 1999;113:249-266.

26 Chen XH, Bezprozvanny I, Tsien RW: Molecular basis of proton block of l-type Ca^{2+} channels. J Gen Physiol 1996;108:363-374.

27 Ankorina-Stark I, Haxelmans S, Hirsch JR, Lohrmann E, Schlatter E: Ca^{2+} entry in isolated rat cortical collecting duct is pH- and voltage sensitive. Cell Physiol Biochem 1997;7:333–344.

28 Sutton RA, Wong NL, Dirks JH: Effects of metabolic acidosis and alkalosis on sodium and calcium transport in the dog kidney. Kidney Int 1979;15:520-533.

29 Dipolo R, Beaugé L: The effect of ph on ca2+ extrusion mechanisms in dialyzed squid axons. Biochim Biophys Acta 1982;688:237-245.

30 Krafte DS, Kass RS: Hydrogen ion modulation of ca channel current in cardiac ventricular cells. Evidence for multiple mechanisms. J Gen Physiol 1988;91:641-657.

31 Polo-Parada L, Korn SJ: Block of n-type calcium channels in chick sensory neurons by external sodium. J Gen Physiol 1997;109:693-702.

32 Ma W, Korngreen A, Weil S, Cohen EB, Priel A, Kuzin L, Silberberg SD: Pore properties and pharmacological features of the p2x receptor channel in airway ciliated cells. J Physiol 2006;571:503-517.

33 Iijima T, Ciani S, Hagiwara S: Effects of the external ph on ca channels: Experimental studies and theoretical considerations using a two-site, two-ion model. Proc Natl Acad Sci USA 1986;83:654-658.

34 Paoletti P, Ascher P, Neyton J: High-affinity zinc inhibition of nmda nr1-nr2a receptors. J Neurosci 1997;17:5711-5725.

35 Hosie AM, Dunne EL, Harvey RJ, Smart TG: Zinc-mediated inhibition of gaba(a) receptors: Discrete binding sites underlie subtype specificity. Nat Neurosci 2003;6:362-369.

36 Huidobro-Toro JP, Lorca RA, Coddou C: Trace metals in the brain: Allosteric modulators of ligand-gated receptor channels, the case of atp-gated p2x receptors. Eur Biophys J 2008;37:301-314.

37 Gore A, Moran A, Hershfinkel M, Sekler I: Inhibitory mechanism of store-operated Ca^{2+} channels by zinc. J Biol Chem 2004;279:11106-11111.

38 Hargitai D, Pataki A, Raffai G, Füzi M, Dankó T, Csernoch L, Várnai P, Szigeti GP, Zsembery A: Calcium entry is regulated by Zn^{2+} in relation to extracellular ionic environment in human airway epithelial cells. Respir Physiol Neurobiol 2010;170:67-75.

39 Linley JE, Simmons NL, Gray MA: Extracellular zinc stimulates a calcium-activated chloride conductance through mobilisation of intracellular calcium in renal inner medullary collecting duct cells. Pflugers Arch 2007;453:487-495.

40 Inagaki A, Yamaguchi S, Takahashi-Iwanaga H, Iwanaga T, Ishikawa T: Functional characterization of a ClC-2-like Cl^- conductance in surface epithelial cells of rat rectal colon. J Membr Biol 2010;235:27-41.